Computational Methods for Color vision.

Synonyms: Color Computational vision, computational neuroscience of color.

Definition

The study of color vision has been aided by a whole battery of computational methods that attempt to describe the mechanisms that lead to our perception of colors in terms of the information processing properties of the visual system. Their scope is highly interdisciplinary, linking apparently dissimilar disciplines such as mathematics, physics, computer science, neuroscience, cognitive science, and psychology. Since the sensation of color is a feature of our brains, computational approaches usually include biological features of neural systems in their descriptions, from retinal light-receptor interaction to sub cortical color opponency, cortical signal decoding and color categorization. They produce hypotheses that are usually tested by behavioral or psychophysical experiments.

Detailed Description

Although the sensation of hue is an invention of our brains, it nevertheless allows us to identify objects by one of their key physical features: their color. Our cortical neurons receive information about the world “out there” and process it in highly non-linear ways to make sense of the environment, highlighting and grouping important items over the rest. In the case of color, this information is carried by the distribution of energy in the photons (wavelength distribution) of the light reflected by objects. Our visual system captures these photons through a very sophisticated mechanism in our retinas, one that converts wavelength information into neural spikes, and ultimately into the vivid sensation we experience. However, the result of this process bares only a small resemblance to the physical characteristics of the light originally falling on our retinas. For instance two objects whose reflected light may differ by only a few more energetic photons may be assigned completely different color categories by our brain. The opposite may also occur: two objects reflecting remarkably different photon/energy distributions may look as having the same color to us. Our perception of color at a point in space may depend not only on the physical characteristics of the light reflected from that point but also on that of the points surrounding it. The origins of these mechanisms are deeply rooted in the lifestyles of our primate ancestors and their need to avoid predators, find

suitable mates and forage for nutritious fruits and leaves in the African forest. These tasks and a changing visual environment may have determined the properties of our color vision and its drive to collect information about the part of the environment that changes the least: the surfaces of objects. This knowledge may help categorize the objects (edible? dangerous?) and therefore improve our chances of survival. In view of this it is easy to understand why our brain has evolved its non-linearities to favor a representation of the world that enhances and improves on the mere physics of the visual environment.

The very properties that aid survival also make the problem of predicting color sensation from the wavelength patterns of light stimulating our retinas very complex and mathematically difficult to address. Color vision scientists have made a great deal of advance, making sense of what is in essence a complex non-linear problem. Each sub-discipline studies the phenomenon from its own unique perspective, with computational approaches contributing to our understanding at every level, from neurophysiology to behavior.

The retina.

The retina is perhaps the best known part of our visual system. It contains three types of photoreceptors or cones that are selectively stimulated by photons according to their energy (wavelength). These receptors (named *L*, *M* and *S* because of their preferences for long, medium and short wavelengths) are light sensitive neurons which fire electrical impulses when exposed to light of wavelengths near their preferred value. Their sensitivity has been quantified [1] in the form of three spectral sensitivities functions (see Figure 1). Notice that since each of the cones could be stimulated by photons with energies within a wide range, long-wavelength preferring cones could be stimulated by medium-wavelength light, etc. Given that cones also respond to light intensity, intense light of sub-optimal wavelength can produce the same firing rate as low intensity light of optimal wavelength. This is the reason why many (in fact infinite) wavelength distributions can produce similar outputs from the cones. Two lights of different wavelength distributions that produce the same retinal output are called *metamers*.

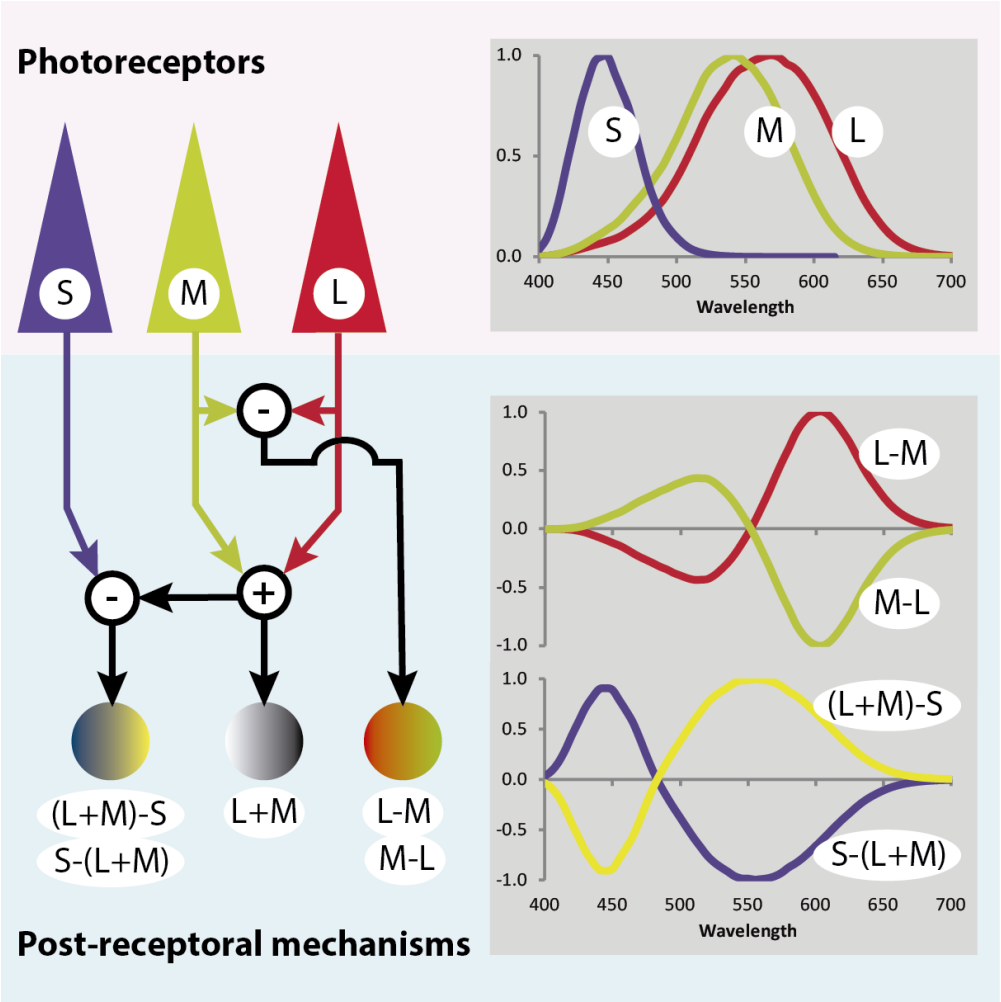

Figure 1. Schematics of the chromatic signal processing in the retina. The figure on the left shows the three human photoreceptors and how they connect to form the three post-receptoral mechanisms by addition and subtraction. Chromatic information is obtained by sampling the spectrum around different wavelengths and comparing the output of at least two different types of photosensitive neurons. Two of the post-receptoral mechanisms are chromatically opponent and one (L+M) is achromatic. Panels on the right show the spectral sensitivity of each chromatic mechanism. The terms L+M, L-M, etc. refer to the sign of the operation and do not represent the weight of each mechanism in the sum.

Receptoral and post-receptoral mechanisms were anticipated in the nineteenth century (well before any physiological observation) in the form of a trichromatic theory by Young [2] and Helmholtz [3] and a color opponent theory by Hering [4]. The first, postulates that color vision is based on three fundamental mechanisms as illustrated at the top of Figure 1 and the second postulates that color vision arises from the workings of three opposed mechanisms: red-green, blue-yellow and light-dark (see bottom of Figure 1). Each theory was an attempt to explain different phenomena such as how mixtures of colored light create a different color or the observation that some opposing pairs of sensations cannot be simultaneously experienced (e.g. there is no reddish-green color), and afterimages (illusory colors that appear after our retinas have been overexposed to colored stimuli) [5]. Our current knowledge of the interaction between cone photoreceptors and light can be expressed mathematically as the integral of the product between the electromagnetic power distribution of the

light and each of the cones' spectral sensitivity functions (*L*, *M* and *S* curves shown in Figure 1).

$$\varepsilon_i = \int_\lambda S_i(\lambda)\ P(\lambda)\ d\lambda \qquad (1)$$

In equation 1 ε_i represents the excitations of the three classes of cones (*i* = *L, M, S*), $S_i(\lambda)$ is their corresponding spectral sensitivity and $P(\lambda)$ is the spectral power distribution of the light falling on them. Since in real life, light measurements are only available at a series of finite wavelengths, the integral in equation 1 is generally approximated to a finite sum over the visible spectrum (400 – 700 nm).

Computational methods for the retina.

In practice, it is unlikely that we know the full spectrum of the light falling on the retina. It is more common to operate retinal models based on images obtained by commercial cameras. These are also modeled by equation 1, but their sensor sensitivities are usually unknown. Some devices are capable of producing images in standard, device-independent color spaces such as the CIE1931 XYZ system or the sRGB color standard, which are easily convertible following a simple set of formulae [6, 7]. Once we know the XYZ coordinates we can obtain the chromaticity coordinates x, y using the following:

$$x = \frac{X}{X+Y+Z} \qquad y = \frac{Y}{X+Y+Z} \qquad (2)$$

From there, it is possible to obtain the cone excitations using Y (luminance) and the following transformation [8]:

$$\begin{aligned} \varepsilon_L &= Y[0.15514\ x/y + 0.54312 - 0.03286(1-x-y)/y] \\ \varepsilon_M &= Y[-0.15514\ x/y + 0.45684 + 0.03286(1-x-y)/y] \\ \varepsilon_S &= Y[0.00801\ (1-x-y)/y] \end{aligned} \qquad (3)$$

In the case of equation 3, ε_i values correspond to the Smith and Pokorny cone fundamentals [9] and the chromaticities ought to be derived from the Judd-modified CIE1931 standard color matching functions [10]. The plot at the top of Figure 1 shows an example of cone fundamentals, with the sensitivity of each cone plotted as a function of wavelength. Color matching functions are obtained from psychophysical experiments where subjects have to visually match the sensation produced by spectrally narrowband stimuli to a mixture of three spectrally broadband lights. It is possible to mathematically obtain cone

fundamentals from such experiments, given certain assumptions [11]. Although Smith and Pokorny did not specify the coefficient necessary to obtain ε_S, the value of 0.00801 was chosen to take into account the relative strengths of the two postreceptoral neural opponent mechanisms (see below).

Equation 3 provides a good approximation for transforming the output of cameras and monitors once we can express it in the CIE1931 XYZ system. However, in most cases this is not possible and devices such as cameras and monitors need to be characterized to convert their outputs to cone excitations. There are several methods for characterizing cameras which include gamut mapping between a known target and the camera output [12, 13], estimation of the camera's sensor sensitivities [14, 15], and mixtures [13] etc. They transform the output of a commercial digital camera into a device-independent color space such as the CIE1931 XYZ.

Receptoral gain control mechanisms.

In the retina, there is a non-linear relationship between the input and the output of the cone photoreceptors, which is often characterized as a gain control mechanism (output signals are modified by signals from the same or different cones). This mechanism converts cone excitations into a contrast representation such as:

$$C_i = \frac{\Delta\varepsilon_i}{\varepsilon_i^b - \varepsilon_i^0}\ ; \qquad i = L, M, S \tag{4}$$

where ε_i^b represents the cone excitation produced by the background (the adaptation state), ε_i^0 is a constant and $\Delta\varepsilon_i$ represents the excitation difference between the cone considered and the background [16]. The *i* sub index discriminates between the three types of photoreceptors.

One of the reasons for this normalization is to reduce the massive intensity range present in the visual environment (in a typical sunny day variations in intensity between shaded and illuminated objects can reach 9 orders of magnitude), which cannot be encoded directly by the output of single neurons (e.g. retinal neurons can encode ranges of approx. 50 to 1) [17].

Post-receptoral color processing

The signals transmitted by cones are combined and encoded in a series of steps by neurons in the retina (the last processing layer is formed by neurons called ganglion cells) and transmitted to an area inside the thalamus called the lateral geniculate nucleus (LGN). The majority of these signals (80% of the fibers reaching the LGN) passes through a layer of ganglion cells called *parvocellular* (or parvo) [17]. At this stage, the information is organized both spatially and chromatically in opponent signals. For example, a parvo cell in the

central retina may receive input from a single L or M cone and weight it against input from a small group of surrounding cones (see Figure 2).

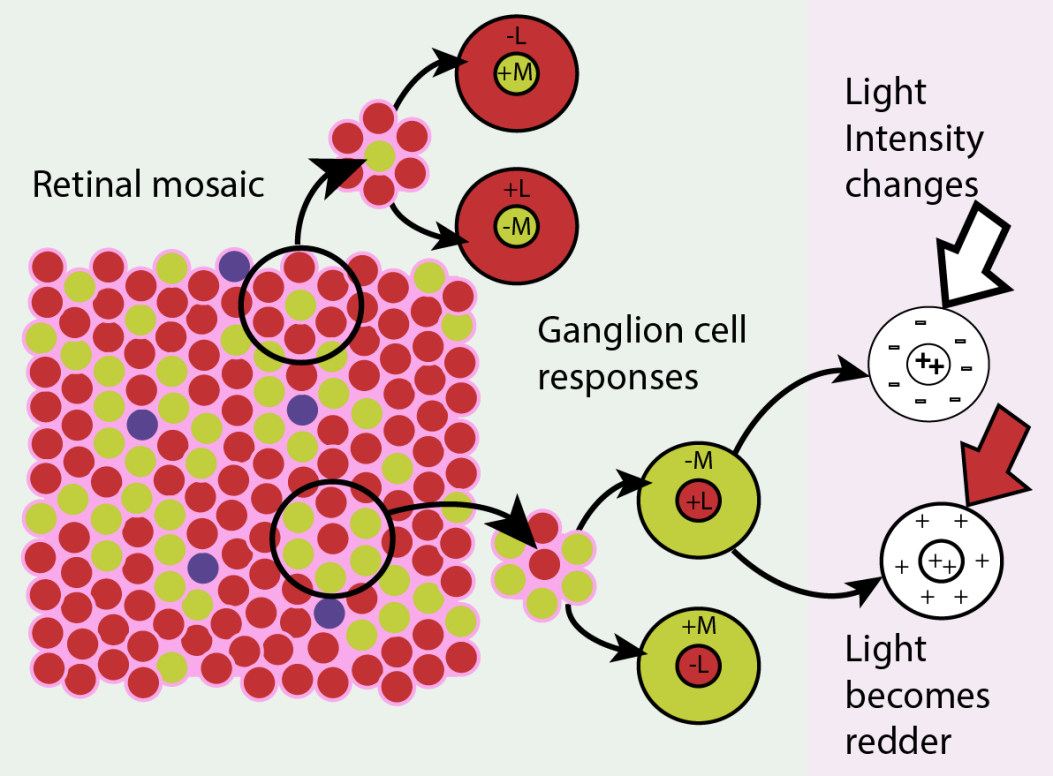

Figure 2: Schematics of the spatiochromatic opponent processing in the retina. Parvocellular ganglion cells collect input from a single cone and compare it with a pool of surrounding cones. In the case of L-M opponency, this leads to four possible combinations, as illustrated in the figure. The right part of the figure shows an example of how the same cell can carry information about both intensity and color. If the light falling on the cell's receptive field changes its intensity, both centre and surround are stimulated, therefore increasing their antagonism. If the same light changes its color towards red, the centre is stimulated and the surround is depressed, contributing less to reduce the ganglion cell output signal (therefore the + sign).

Each ganglion cell is stimulated by light falling on a physical part of the retina that contains the cones to which it is connected (its receptive field). As a result of the wiring shown in Figure 2, parvo cells output a signal that is spatially and chromatically opponent and conveys both intensity (i.e. brightness) and wavelength information (i.e. color) from the light falling on its receptive field. Thus parvo cells perform a 'double-duty', carrying information about both intensity and color. The right part of Figure 2 shows how intensity changes in light increase the cell's antagonism, conveying information about the smallest possible unit (a cone) while chromatic changes produce a synergistic response in the center and surround, thus increasing the number of cones contributing to the signal. For this reason, parvo cells in Figure 2 convey finer detail information (higher spatial frequencies) about intensity than for color. In other words, when light varies spatially in color, the same cells can only carry information about its coarse spatial distribution (lower spatial frequencies). This imbalance has been confirmed psychophysically by our greater ability to detect fine patterns of achromatic light and coarse patterns of colored light [18], and matches the information content of natural scenes [19]. This combination of spatial and

chromatic opponency in parvo cells appears to be a sophisticated mechanism to optimally extract information from the visual environment, carrying both chromatic and achromatic signals over different spatial frequency bands (multiplexing).

Computationally, it is common to model the centre-surround receptive field structure by convolving the color opponent representations with Gaussians kernels of opposite sign and different standard deviations (difference of Gaussians). For example, one kernel is applied to the L cone representation and another (of greater standard deviation) to the M cone representation and the results subtracted from each other. This process is equivalent to subtracting a blurred version of the M-cone excitation image (the surround) from another, slightly blurred version of the L-cone excitation (the centre). A similar algorithm can be applied to obtain S-(L+M) opponency. Similarly to parvo, there exist in the retina two other types of ganglion cells. The *Koniocellular* (or konio) cells that carry information about S cones excitation relative to their surrounds (S-(L+M) and –S+(L+M)) and the *Magnocellular* (or magno) that receive excitatory output from all three types of cones, therefore is insensitive to color [17]. Figure 1 illustrates this opponency from a spectral point of view.

Sub cortical color representations

The three types of ganglion cells described above connect to specialized layers of neurons in the LGN. The presence of these LGN cells representing different aspects of the light captured by cones has inspired the creation of color spaces based on the properties of these neurons. The best known is the MacLeod-Boynton cone excitation space [20] which is based on the coefficients of equation 3 plus an arbitrary condition that the relationships among the sensitivities of the three receptoral mechanisms at 400 nm (see Figure 1) will be given by equation 5:

$$S_L(400) + S_M(400) = S_S(400) \tag{5}$$

where $S_i(400)$ is the sensitivity of each cone photoreceptor at 400 nm. To obtain the coordinates of the MacLeod-Boynton receptor space it is necessary to convert the *L*, *M*, *S* cone excitations to coordinates *l*, *m*, *s* using the following transformation:

$$l = \frac{L}{L+M}; \quad m = \frac{M}{L+M}; \quad s = \frac{S}{L+M} \tag{6}$$

The normalization provided by equation 5 constrains the value of *s* in equation 6 between 0 and 1.

An extension of cone-excitation spaces are cone-contrast spaces, which address the issues posed by the receptoral gain control mechanisms described in equation 4. Two popular cone-contrast spaces were created by Derrington *et al* [21] and Boynton [22] following different assumptions about the neutral points (crossings of the L-M and S-(L+M) functions of Figure 1). Cone-contrast representations take into account the cone excitation produced by the background, and re-scale the signal accordingly. The new coordinates become:

$$\mathrm{C_i} = \frac{\Delta\varepsilon_i}{\varepsilon_\mathrm{i}^\mathrm{b}}; \qquad \mathrm{i} = \mathrm{L, M, S} \tag{7}$$

where $\Delta\varepsilon_i$ is the cone-excitation difference between the signal and a given reference level (the background). $\varepsilon_\mathrm{i}^\mathrm{b}$ is the cone excitation produced by the background. In this new representation, the background excitation becomes the origin of the new system. Cone contrast spaces provide a representation of the input signal arriving at later stages in the visual pathway.

Cortical color processing

LGN neurons project to the primary visual cortex in the occipital part of the brain (also known as striate cortex or area V1). From there, visual information is sent to the so called extrastriate visual cortical areas (named V2, V3, V4, and V5). Each part of the retina is mapped into V1 with a very precise correspondence between the visual field and its related location in the primary visual cortex. A large portion of V1 is dedicated to the center of the retina, where the abundance of cones is highest and the receptive field smallest. In contrast to the well defined, opponent-color information carrying neurons found in the retina and LGN, color sensitive cortical neurons respond to many other properties of the visual stimulus such as contrast, object orientation, shape, etc. This is thought to be the reason behind many illusory phenomena where the color of the area we gaze is influenced by patterns of the surrounding area (chromatic induction, see Figure 3) and color constancy [23].

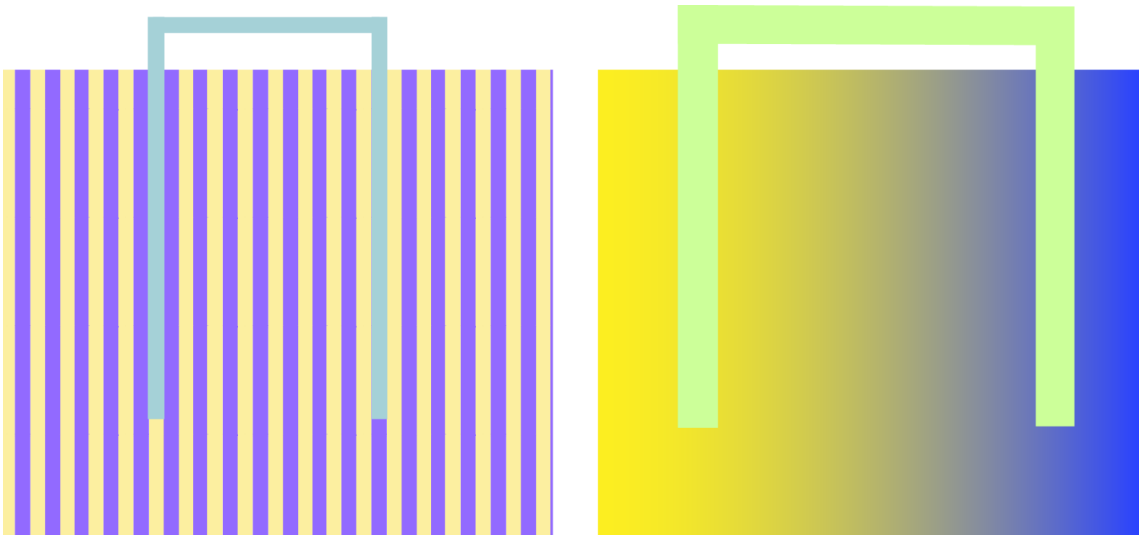

Figure 3 shows the influence of surrounding patterns on the perceived color of a central area. In both figures, the inverted "U" bar has the same RGB values but it is perceived differently according to its surroundings. This phenomenon is called "chromatic induction".

Originally, color processing in the visual cortex was thought to be modular and separated from other forms of perception. This view was supported by studies in cerebral achromatopsia (a lesion in the brain that causes loss of the ability to recognize colors without loss of form and motion perception) and others [24]. Today's prevalent view is that V1 is strongly stimulated by color, with about 50% of its neurons responsive to some kind of chromatic stimulus, with L-M being the preferred direction [25]. Areas V2 and V4 also respond to color, however, many of their neurons respond equally to achromatic patterns. Two intriguing classes of color processing neurons were found in the primary visual cortex: single- and double-opponent cells [25, 26] (see Figure 4). The former respond best to large areas of color while the later have preference for color boundaries, patterns and textures. Both types of neurons have been linked to the perceptual phenomena shown in Figure 3.

There have been reports in the literature about a spatial segregation of color-selective neurons in V1 and V2. A number of optical imaging electrophysiological and microelectrode studies have found the presence of clusters of color selective neurons, although there are still negative results and the issue has not been definitively resolved [25].

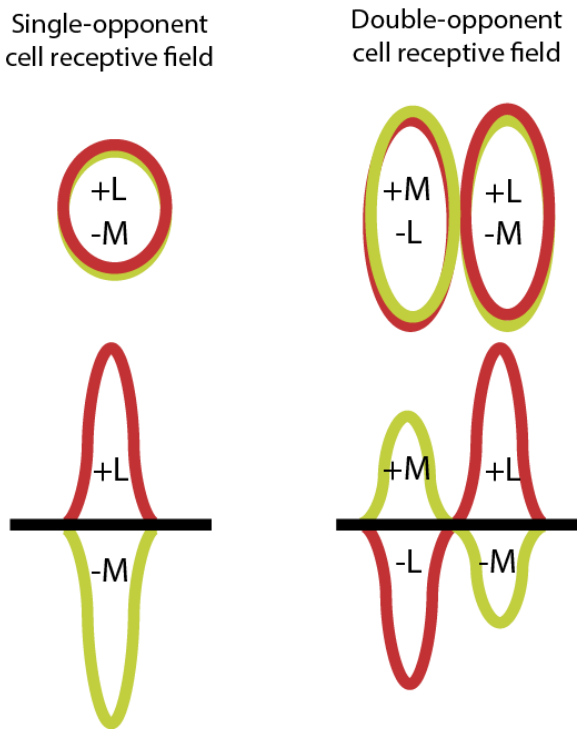

Figure 4: Cartoon examples of single-opponent and double-opponent color processing cells. Single-opponent cells are insensitive to edges and do not prefer any oriented stimuli. They respond strongly to colored patches. On the other hand, double-opponent cells are strongly selective for chromatic edges and have a preferred orientation.

Computational models of color processing in the visual cortex.

Computational models of cortical processing can be categorized as either primarily phenomenological, i.e. trying to capture the observed phenomena in a convenient mathematical form, or mechanistic, i.e. trying to show how observed phenomena arise from biologically grounded neural mechanisms. A typical color vision model contains a pre-processing stage where the input image is converted to a L, M, S cone excitation representation, a cone opponency stage that weights the output of cones to produce opponent signals and other post-receptoral stages which may include normalizations by neighboring units and weighting parameters. The centre-surround receptive field interaction is usually modeled via a pyramid of 2-dimensional Gaussians or Gabor operators that convolve the image to obtain chromatic and achromatic information at different spatial scales and orientations. A final layer can also be implemented to account for single- and double-opponent cell processing.

Chromatic induction demonstrations like those shown in Figure 3 have inspired some computational attempts to model color processing in the visual cortex, trying to predict the effects of surround stimuli on the perceived color of a central patch. Examples of these are the models of Singer & D'Zmura [27], Spitzer and Barkan's model [28] and Otazu *et al's* CIWaM [29]. The later consists of a cone receptor stage that separates the input into two chromatic and one achromatic channel, a wavelet pyramid to model spatiochromatic processing in the cortex, including normalization effects by neighboring neurons

(divisive normalization) [30], and a weighting function to mimic the spatial filtering of the human visual system. A later version of CIWaM was capable of predicting unconstrained eye movements in human subjects [31].

A family of computational approaches to color processing takes advantage of the tools currently available in computer science for tasks such as object recognition. For example, one approach consists of applying shape-based descriptors such as Scale-invariant feature transform (Sift) on the post-receptoral color representations. Sift will learn “interesting features” of an object in a set of training images which can be later used to identify the object in the dataset. Other approaches involve a set of shape-based descriptors computed from grayscale pixel intensities, which are in turn concatenated with hue histograms. An improvement has been proposed by Van de Weijer and Schmid who concatenated a hue histogram with grayscale Sift image descriptors [32] while Zhang *et al* [33] described a hierarchical model of color processing inspired in the primate visual cortex. They produced chromatically opponent channels using operators that resemble single- and double- opponent cells and outperformed the object recognition previous approaches.

Color constancy

The human visual system has the ability to perceive objects as having a well defined color despite the fact that they reflect light according to their own pigmentation, geometry and the wavelength content of the illumination. During a typical day, natural daylight changes its color quite dramatically but we are mostly unaware of its full effect on the surfaces of objects. As we have seen before, the distribution of power as a function of wavelength in the light reaching our retinas determines how we perceive color. In the case of light reflected from objects, this power distribution depends of several factors. Equation 8 provides a simplified description of the problem [23]:

$$\mathrm{C}(\lambda) = \mathrm{E}(\lambda)\mathrm{R}(\lambda) \qquad (8)$$

Here $\mathrm{C}(\lambda)$ is the spectral power distribution of the light reaching our retina, $\mathrm{E}(\lambda)$ is the spectral power distribution of the illumination and $\mathrm{R}(\lambda)$ is the spectral reflectance of the surface. Equation 8 assumes that the illumination is spatially uniform and surfaces are Lambertian (diffusely reflective, with no specularities). Of these factors, only $\mathrm{R}(\lambda)$ is intrinsic to the objects while $\mathrm{E}(\lambda)$ changes according to the type of illumination, physical location, time of the day, etc. In summary, to produce a stable scene in terms of color, the human visual system disentangles the two factors at the right side of the Equation 8. This is a mathematically ill-posed problem, given that there are infinite possible combinations of illumination and reflectance that produce the same reflected light. To solve it, the human visual system may resort to information from

previous experience, scene features such as specular reflections and interreflexions and memory of colors, etc.

The problem of illumination removal is ubiquitous. For example, in computer vision there are applications that require illumination stability in order for algorithms to work. In photography, users expect the image to represent the scene “as they saw it” not the actual physical values. Many popular computational approaches try to solve this problem by taking into account the information intrinsic to the image, rather than the physiological or anatomical mechanisms of the visual system. For practical reasons, methods were developed to return an image that approximately represents the intrinsic color of objects, discounting the effects of the illumination (canonical image). This image can be then “reilluminated” to create conditions close to the observer’s perception. Illuminant-removal methods contain different statistical hypothesis, being the most popular the “grey world” assumption, which states that the *average reflectance of a scene is achromatic*. Another popular hypothesis (called “MAX-RGB”) takes advantage of some properties of white surfaces and specular reflections, and is based on the assumption that *the maximum reflectance of a scene is achromatic*. Once a hypothesis is introduced, the computational algorithm returns an image that meets the hypothesis. Many of these solutions are strongly dependent on whether the input image complies with the hypothesis and are prone to fail in particular cases. For example, a “grey world” algorithm may fail when the average color of the scene is not grey. The main drawback of this family of computational approaches is that they do not provide much insight about the mechanisms that are behind color constancy. See Gevers *et al* [32] for a comparison of illuminant-removal methods.

Color appearance

The models and the physiologically-based color spaces described above have been created to handle the perception of colors viewed in isolation and in controlled, fully adapted conditions. However, the perceptual appearance of colors in naturalistic viewing conditions depends of so many external factors (surround, background, illuminant, etc.) that a series of sophisticated models have been created to account for them. These so called color appearance models are not constrained by attempts to incorporate elements of the physiology [34].

References

[1] A. Stockman, L.T. Sharpe, The spectral sensitivities of the middle- and long-wavelength-sensitive cones derived from measurements in observers of known genotype, Vision Research, 40 (2000) 1711-1737.
[2] T. Young, On The Theory Of Light And Colours, Philosophical Transactions of the Royal Society of London, 92 (1802) 12-48.

[3] H.v. Helmholtz, Handbuch der physiologischen Optik, Voss, Leipzig,, 1867.
[4] E. Hering, Zur Lehre vom Lichtsinne. Sechs Mittheilungen an die Kaiserl. Akademie der Wissenschaften in Wien. , 2 ed., Gerold, Wien, 1875.
[5] R.L. Gregory, Seeing colours, in: Eye and brain : the psychology of seeing, Oxford University Press, Oxford, 1998, pp. 121-134.
[6] C.A. Poynton, Digital video and HDTV : algorithms and interfaces, Morgan Kaufmann Publishers, Amsterdam ; Boston, 2003.
[7] P. Green, L. MacDonald, Colour engineering : achieving device independent colour, Wiley, Chichester, 2002.
[8] G. Wyszecki, W.S. Stiles, Theories and models of color vision, in: Color science : concepts and methods, quantitative data and formulae, Wiley, New York ; Chichester, 1982, pp. 615.
[9] V.C. Smith, J. Pokorny, Spectral sensitivity of the foveal cone photopigments between 400 and 500 nm, Vision Research, 15 (1975) 161-171.
[10] D.B. Judd, Report of U.S secretariat committee on colorimetry and artificial daylight, in: Twelfth Session of the CIE, Bureau Central de la CIE, Stockholm, 1951, pp. 11.
[11] G. Wyszecki, W.S. Stiles, Colorimetry, in: Color science : concepts and methods, quantitative data and formulae, Wiley, New York ; Chichester, 1982, pp. 117-145.
[12] V. Cheung, S. Westland, D. Connah, C. Ripamonti, A comparative study of the characterisation of colour cameras by means of neural networks and polynomial transforms, Coloration Technology, 120 (2004) 19-25.
[13] C.A. Parraga, R. Baldrich, M. Vanrell, Accurate Mapping of Natural Scenes Radiance to Cone Activation Space: A New Image Dataset, in: CGIV 2010/MCS'10 - 5th European Conference on Colour in Graphics, Imaging, and Vision - 12th International Symposium on Multispectral Colour Science, Society for Imaging Science and Technology Joensuu – Finland, 2010, pp. 50-57.
[14] S. Westland, C. Ripamonti, Caracterization of Cameras, in: Computational colour science : using MATLAB, Wiley, Chichester, 2004, pp. 127-128.
[15] K. Barnard, B. Funt, Camera characterization for color research, Color Research and Application, 27 (2002) 153-164.
[16] A. Stockman, D.H. Brainard, Color vision mechanisms, in: M. Bass, V.N. Mahajan (Eds.) OSA Handbook of Optics, McGraw-Hill, New York, 2010, pp. 11.11 - 11.104.
[17] R. De Valois, Neural Coding of Color, in: J.S. Werner, L.M. Chalupa (Eds.) The visual neurosciences, MIT Press, Cambridge, Mass., 2004, pp. 1001.
[18] R.L. De Valois, K.K. De Valois, Spatial vision, Oxford University Press, New York, 1988.
[19] C.A. Parraga, T. Troscianko, D.J. Tolhurst, Spatiochromatic properties of natural images and human vision, Current Biology, 12 (2002) 483-487.
[20] D.I.A. MacLeod, R.M. Boynton, Chromaticity diagram showing cone excitation by stimuli of equal luminance, Journal of the Optical Society of America, 69 (1979) 1183-1187.
[21] A.M. Derrington, J. Krauskopf, P. Lennie, Chromatic Mechanisms in Lateral Geniculate-Nucleus of Macaque, Journal of Physiology-London, 357 (1984) 241-265.
[22] R.M. Boynton, A system of photometry and colorimetry based on cone excitations, Color Research and Application, 11 (1986) 244-252.
[23] D.H. Brainard, Color Constancy, in: L.M. Chalupa, J.S. Werner (Eds.) The visual neurosciences, MIT Press, Cambridge, Mass., 2004, pp. 948-961

[24] S. Zeki, A vision of the brain, Blackwell Scientific Publications, Oxford ; Boston, 1993.
[25] R. Shapley, M.J. Hawken, Color in the Cortex: single- and double-opponent cells, Vision Research, 51 (2011) 701-717.
[26] A. Hurlbert, Colour vision: Primary visual cortex shows its influence, Current Biology, 13 (2003) R270-R272.
[27] B. Singer, M. D'Zmura, Contrast gain control: a bilinear model for chromatic selectivity, J Opt Soc Am A Opt Image Sci Vis, 12 (1995) 667-685.

[28] H. Spitzer, Y. Barkan, Computational adaptation model and its predictions for color induction of first and second orders, Vision Research, 45 (2005) 3323-3342.
[29] X. Otazu, C.A. Parraga, M. Vanrell, Towards a unified model for chromatic induction, Journal of Vision, 10 (2010) 5 1-24.
[30] D.J. Heeger, Normalization of cell responses in cat striate cortex, Visual Neuroscience, 9 (1992) 181-197.
[31] N. Murray, M. Vanrell, X. Otazu, C.A. Parraga, Saliency estimation using a non-parametric low-level vision model, in: Computer Vision and Pattern Recognition (CVPR), 2011 IEEE Conference on, 2011, pp. 433-440.
[32] T. Gevers, Color in computer vision : fundamentals and applications, Wiley, Hoboken, NJ, 2012.
[33] J. Zhang, Y. Barhomi, T. Serre, A New Biologically Inspired Color Image Descriptor, in: A.W. Fitzgibbon, S. Lazebnik, P. Perona, Y. Sato, C. Schmid (Eds.) ECCV 2012 - 12th European Conference on Computer Vision, Springer, Florence, Italy, October 7-13, 2012, pp. 312-324.
[34] M.D. Fairchild, Color appearance models, Addison-Wesley, Reading, Mass. ; Harlow, 1998.